Simple Defocus Laser Irradiation to Suppress Self-Absorption in Laser-Induced Breakdown Spectroscopy (LIBS)

Alion Mangasi Marpaung
Jakarta State University
Edward Harefa
Zhejiang Normal University
Marincan Pardede
University of Pelita Harapan
Indra Karnadi
Krida Wacana Christian University
Rinda Hedwig
Bina Nusantara University
Ivan Tanra
Krida Wacana Christian University
Maria Margaretha Suliyanti
Indonesia Institute of Science
Zener Sukra Lie
Binus ASO school of engineering
Muhandis Shiddiq
Indonesia Institute of Science
Muliadi Ramli
Syiah Kuala University
Kurnia Lahna
Syiah Kuala University
Eric Jobiliong
University of Pelita Harapan
Syahrun Nur Abdulmadjid
Syiah Kuala University
Nasrullah Idris
Syiah Kuala University
Ali Khumaeni
Diponegoro University
Wahyu Setiabudi

Diponegoro University

Hery Suyanto

Udayana University

Tjung Jie Lie

Research Center of Maju Makmur Mandiri Foundation

Koo Hendrik Kurniawan (kurnia18@cbn.net.id)

Research Center of Maju Makmur Mandiri Foundation

Kiichiro Kagawa

Fukui Science Education Academy

Research Article

Keywords: self-reversal emission lines, self-absorption, resonant lines, defocus laser irradiation, LIBS

Posted Date: December 17th, 2021

DOI: https://doi.org/10.21203/rs.3.rs-1150326/v1

Abstract

This study introduces a novel and extremely simple way for suppressing the self-absorption effect in laser-induced breakdown spectroscopy (LIBS) by utilizing a defocusing laser irradiation technique. It is claimed that defocusing laser irradiation produces more uniform laser plasma due to lower fluence than tight focus laser irradiation, hence greatly lowering the effect of self-absorption in the laser plasma. KCl and NaCl pellet samples were used to demonstrate this achievement. When the defocus position is adjusted to – 6 mm for KCl and NaCl samples, the self-reversal emission lines K I 766.4 nm, K I 769.9 nm, Na I 588.9 nm, and Na I 589.5 nm vanish. Meanwhile, the FWHM values of K I 766.4 and K I 769.9 nm are 0.29 nm and 0.23 nm, respectively, during -6 mm defocus laser irradiation, as opposed to 1.24 nm and 0.86 nm, under tight focus laser irradiation. Additionally, this work demonstrates that when the laser energy is changed in between 10 to 50 mJ, no self-reversal emission occurs when -6 mm defocus laser irradiation is applied. Finally, a linear calibration curve is generated using KCl at a high concentration ranging between K concentration from 16.6–29%. This simple change of defocus laser irradiation will undoubtedly contribute to the suppression of the self-absorption phenomenon, which disrupts LIBS analytical results.

Introduction

We discover that the number of publications in the field of LIBS has not dropped during the COVID-19 pandemic, which is approaching two years and has been accompanied by lockdowns in practically all universities and research centers worldwide. This demonstrates that LIBS as an analytical technology continues to pique the interest of scientists all over the world. LIBS research has primarily taken two paths since its discovery in the early 1980s. The first is on the basic aspects of the LIBS plasma, such as plasma dynamics, electron number density, plasma temperature, line broadening and line shift, and plasma modeling.[1–7] Second, it is primarily concerned with its numerous applications, which include qualitative and quantitative material analysis[8–11], biological applications such as clinical specimens such as human blood[12,13], surface analysis including depth profile measurement[14–17], isotopic analysis[18–20], and many other interesting LIBS applications that are not discussed in detail in this paper.

Despite its popularity as a versatile analytical tool, LIBS still suffers from the self-absorption effect, especially for emission lines originating from direct resonant transition involving the ground state. The existence of this effect causes the failure to obtain a linear calibration curve, which is very needed for reliable quantitative analysis. Many researchers have proposed excellent techniques to overcome or minimize this problem. Ran Hai et al[21] applied the argon atmosphere and selection of the time window for the detection system to minimize self-absorption. Zhang Xiong et al[22] used the fiber laser to suppress the self-absorption in Mg and Ca emission lines. Yun Tang et al[23,24] found that the detection window of 0.2 – 0.4 μs can produce a linear calibration curve for Mn. They also proposed to use a microwave-assisted excitation in LIBS (MAE-LIBS) to reduce the effect of self-absorption in a wide spectral range of 200 – 900 nm. Another impressive work, performed by Jia Ming et al[25] employing LIBS assisted by laser-

stimulated absorption (LSA-LIBS) can significantly reduce the self-absorption in K, Mn, and Al. Another approach to suppress the effect of self-absorption by using a mathematical model was also carried out by Cristoforetti et al[26], Aragon et al[27], and Safi et al[28]. However, their mathematical complexity limited the application. There are many more studies on how to suppress the effect of self-absorption in LIBS which cannot be mentioned one by one in this paper[29–34], but one can find the references that are mentioned in this paper.

To suppress the self-absorption effect in LIBS, we proposed the use of a He metastable excited state to excite the ablated target atoms in our prior work on the subject.[35] It was discovered that the elements K, Na, and Al emit free self- reversal emissions lines. For those elements, a linear calibration curve was also obtained. Furthermore, we developed a double pulse orthogonal approach, with which we were able to create emission lines with high concentrations of K, Na, and Al that were practically free of self-reversal and only moderately impacted by the self-absorption phenomenon.[36] Similarly, we recently proposed parallel laser irradiation to minimize the self-absorption phenomenon and we were able to achieve emission lines of K that were practically free of self-reversal.[37]

Although all the techniques described above produce good results for suppressing self-absorption in LIBS, they are all faced with a significant amount of complexity, including the need to use two lasers, the use of a time-resolved measurement that will reduce the emission intensity to the point where the S/N becomes poor, and the use of a mathematical model to compensate for the self-absorption effect. To address this, we present a novel method for suppressing the self-absorption effect that is both easy and inexpensive, namely defocusing laser irradiation. It has been demonstrated that the created plasma is more homogeneous under defocus laser irradiation than under tight focus laser irradiation, allowing the self-absorption effect to be suppressed as low as possible. Experiments with KCl and NaCl samples revealed free self-reversal emission lines of K I 766.4 nm, K I 769.8 nm, Na I 588.9 nm, and Na I 589.5 nm. Furthermore, even at very high concentrations of KCl, we achieved a linear calibration curve, even though we all know that the higher the element concentration, the greater the self-absorption effect.

Materials And Methods

This experiment uses KCl and NaCl powder from Wako Chemical, Japan, with a purity of 4N. Pellets are formed by pressing the powders under 30 MPa pressure for 90 seconds after they have been ground to around 50 μm grain size. The diameter of the final pellet was 10 mm, while the thickness was 2 mm. Fig. 1 depicts the experimental setup employed in this study. A fundamental Nd:YAG laser (Quanta Ray model LAB 130-10) is the laser utilized in this experiment, which can operate between 9 and 50 mJ by using a neutral density filter. In all the trials, the repetition rate of the laser is set at 10 Hz. A plano-convex quartz lens of 150 mm focal length is utilized to focus the laser irradiation onto the sample surface.

The sample is placed in a sample holder that is attached perpendicular to the servo motor's axis, and the entire set is placed above the x-y-z stages with micrometer adjustment. The servo motor's speed is set to 6 rpm so that each laser irradiation attacks a different place on the sample surface. The emission of the

created atmospheric plasma is collected using a 45-degree optical fiber. The opposite end of the optical fiber is attached to the input slit of a spectrograph (McPherson model 2061, focal length 1000 mm, f/8.6, Czerny Turner configuration), the output slit of which is tied to a gated intensified charge-coupled device (ICCD; Andor iStar intensified CCD, 1,024 x 256 pixels, UK). The synchronized Q-switched laser output is used to trigger the ICCD. The ICCD's gate delay and gate width are fixed at 1 μs and 30 μs, respectively, making it a time-integrated measurement. All the data produced in this work is the average of 20 accumulations of laser irradiation onto the sample surface.

Results And Discussion

Since this study is mainly concerned with the focusing position of the laser irradiation, it is very important to know exactly where the tight focus position is. In this case, we use a pure copper plate (Rare Metallic, 5N, 1 cm diameter, and thickness of 0.4 mm) as a sample. We detect the emission spectra of typical Cu emission lines of Cu I 510.5 nm, Cu I 515.3 nm, and Cu I 521.8 nm as the laser energy decreases to as low as 0.5 mJ. By adjusting the y-direction of the x-y-z stage in which the sample is positioned, we determined the highest emission intensities of the above three Cu lines. This position is then marked as a tight focus position (zero position). It is important to note that shifting 0.1 mm away from the sample surface from the tight focus position yielding almost no emission of the above three Cu lines. From this result, we conclude that the precision of the focusing apparatus used in this study is 0.1 mm. We also noted by our naked eyes that the tiny green plasma of Cu disappears when the focusing position is shifted 0.1 mm from its tight focus position. This is mainly due to the very small energy of the laser irradiation used to determine the tight focus position yielding a very high accuracy of the tight focus position.

Figure 2 shows the emission spectrum of KCl at various focusing positions, including tight focus, +3 mm, -3 mm, -6 mm, -9 mm, and -12 mm. The negative (–) and positive (+) signs denote a position deviation from tight focus (zero) position in y-axis, respectively. The laser energy is fixed at 21 mJ, and the ICCD's gate delay and width are set to 1 μs and 30 μs, respectively. When laser irradiation is performed at a tight focus, a self-reversing emission spectrum of K I 766.4 nm and K I 769.9 nm is observed, and this effect is exacerbated when the focus position is set to +3 mm. When the focus position is shifted to the negative direction (shorter than the lens's focal length), self-reversal emission is significantly reduced. Negligible self-reversal of the K I 769.9 nm emission line is observed at -3 mm. Both K emission lines exhibit a free self-reversal emission line at –6 and –9 mm. Further defocus to –12 mm results in significant self-reversal emission of both K emission lines, as well as a significant reduction in emission intensity. We observed that the best emission spectra for K are observed at –6 mm and –9 mm defocus positions. A similar spectrum is obtained for a NaCl sample, as shown in Fig. 3. The difference between the NaCl and KCl spectra is minimal, with the best focusing position being only –6 mm. According to the results of Figure 2 and Fig. 3, the next experiment will focus exclusively on the –6 mm defocusing position

The reason why the self-reversal effect is greatly reduced in the negative defocus position could be that in the defocus condition, the larger beam waist and more flatter beam profile of the laser irradiation is responsible for the ablation of the sample yielding homogeneous plasma as opposed to tight focus laser

irradiation with a much smaller beam waist on the sample surface. When there is too much negative defocus, such as – 12 mm, the fluence of the laser becomes too small, resulting in a serious self-reversal process. This explanation also applies to + 3 mm defocus because most of the laser energy is used to create air breakdown in front of the sample surface and only a small fraction of the laser energy is used to ablate the sample. Rezaei et al[34] provide a comprehensive study on the relationship between plasma homogeneity and the self-reversal process. In this experiment, the beam waist is 25.4 μm for tight focus and 141 μm for defocus at -6 mm. Meanwhile, the fluence is 0.41 GJ/cm^2 at tight focus and 0.013 GJ/cm^2 for defocus at -6 mm.

The following experiment was carried out to determine the relationship between laser energy and defocus position that produces spectra without self-reversal. This is accomplished by varying the laser energy from 9 mJ, 21 mJ, 33 mJ, and 44 mJ, as shown in Fig. 4. As a sample, a KCl sample is used. Once again, the -6 mm defocus position provides the best spectral results without requiring a self-reversal process for the various energy lasers used. One might wonder why we only use laser energies ranging from 10 to 50 mJ. This is because we hope to use this technique for in-situ analysis soon, and in that case, a small portable Nd:YAG laser with a maximum energy of 50 mJ is easily available on the market.

Various pellet samples with different concentrations of KCl were prepared to determine the linearity of the calibration curve. As a KCl companion, NaCl is used. Fig. 5 shows the KCl calibration curve at 30%, 35%, 40%, 50%, and 55% concentrations which is corresponds to the K concentration of 16.6%, 18.3%, 21%, 26% and 29%. In Fig. 5, the measured K I 766.4 nm and K I 769.9 nm emission intensities are plotted against the associated K concentrations. Each data point in this graph is the average of five data points obtained from 20 successive laser irradiations. Over the dynamical range used in this study, the K concentration and its associated emission intensity show a clear linear relationship with a very high determination coefficient R^2 of 0.99 for K I 769.9 nm and 0.98 for K I 766.4 nm. However, we discovered that the calibration curve is not intercepted at 0 points, which can be explained simply by the high concentration used to obtain the calibration curve. It should also be noted that the K concentration used to generate the calibration curve is extremely high, up to 29%. As a result, the likelihood of self-absorption in the plasma is extremely high. However, the presented calibration curve is still linear, demonstrating that our novel defocus laser irradiation technique is effective in completely suppressing self-absorption in LIBS.

Conclusion

In conclusion, the laser irradiation defocus method developed in this study can suppress the effect of self-absorption on LIBS. The linear calibration curve of KCl at high concentrations demonstrates this. It should also be noted that the spectrum we show is a time-integrated spectrum, which means that a quantitative analysis of the self-absorption-free LIBS method can be performed in field studies by combining a portable laser and a time-integrated CCD, both of which are widely available on the market.

Declarations

Acknowledgments

This work is supported partially through a Basic Research Grant in Physics, The Academy of Sciences for the Developing World, Third World Academy of Sciences (TWAS), under contract number 060150 RG/PHYS/AS/UNESCO FR:3240144882. This project is also partially funded by the Indonesia Ministry of Education, Culture, Research, and Technology through a research grant under decision letter NO:7/E/KPT/2019 and agreement contract NO:22/SP2H/DRPM/LPPM-UNJ/III/2019. The authors express their sincerest thanks to the late Prof. M. O. Tjia for his longstanding guidance.

Author contributions:A.M.M.,I.K., M.P., E.H., T.J.L. and K.K. conceived the experiment(s); M.S., M.M.S., I.T., R.H., M.R., K.L., E.J., S.N.A., N.I., A.K., conducted the experiment(s); H.S., W.S., prepared the samples and figures; I.K., M.P., H.S., T.J.L and K.H.K. analyzed and interpreted the data; K.H.K and I.K. wrote the main manuscript text; K.H.K supervised the whole research. All authors reviewed the manuscript.

Competing interests: The authors declare no competing interests.

References

1. Miziolek, A., Palleschi, V. & Schechter, I. *Laser-Induced Breakdown Spectroscopy (LIBS): Fundamentals and Applications* (Cambridge University Press, 2006).
2. Cremers, D. A. & Radziemski, L. J. *Handbook of Laser-Induced Breakdown Spectroscopy* (John Wiley & Sons, Ltd, 2006).
3. Fortes, F. J., Moros, J., Lucena, P., Cabalín, L. M. & Laserna, J. J. Laser-Induced Breakdown Spectroscopy. *Anal. Chem*, **85**, 640–669 (2013).
4. Budi, W. S. *et al.* Neutral and Ionic Emission in Q-Switched Nd:YAG Laser-Induced Shock Wave Plasma. *Appl. Spectrosc*, **53**, 1347–1351 (1999).
5. Marpaung, A. M., Kurniawan, H., Tjia, M. O. & Kagawa, K. Comprehensive study on the pressure dependence of shock wave plasma generation under TEA CO2laser bombardment on metal sample. *J. Phys. D. Appl. Phys*, **34**, 758–771 (2001).
6. Li, Y. *et al.* A review of laser-induced breakdown spectroscopy signal enhancement. *Appl. Spectrosc. Rev*, **53**, 1–35 (2018).
7. Konjević, N. Plasma broadening and shifting of non-hydrogenic spectral lines: present status and applications. *Phys. Rep*, **316**, 339–401 (1999).
8. Yao, S. *et al.* Optimization of laser-induced breakdown spectroscopy for coal powder analysis with different particle flow diameters. *Spectrochim. Acta Part B At. Spectrosc*, **110**, 146–150 (2015).
9. Bengtson, A. Laser Induced Breakdown Spectroscopy compared with conventional plasma optical emission techniques for the analysis of metals – A review of applications and analytical performance. *Spectrochim. Acta Part B At. Spectrosc*, **134**, 123–132 (2017).

10. Wang, Z., Deguchi, Y., Shiou, F., Yan, J. & Liu, J. Application of Laser-Induced Breakdown Spectroscopy to Real-Time Elemental Monitoring of Iron and Steel Making Processes. *ISIJ Int*, **56**, 723–735 (2016).
11. Wang, F. Z. D. Q. *et al.* C. Recent progress on the application of LIBS for metallurgical online analysis in China. *Frontiers of Physics*, **7**, 679–689 (2012).
12. Rehse, S. J., Salimnia, H. & Miziolek, A. W. Laser-induced breakdown spectroscopy (LIBS): an overview of recent progress and future potential for biomedical applications. *J. Med. Eng. Technol*, **36**, 77–89 (2012).
13. Khumaeni, A., Setia Budi, W., Wardaya, A. Y., Hedwig, R. & Kurniawan, K. H. Elemental characterization of human blood using Laser-Induced Breakdown Spectroscopy utilizing 355 nm Nd: YAG operated at reduced pressure of He gas. *Rasayan J. Chem*, **14** (4), 2413–2419 (2021).
14. Pouli, P., Melessanaki, K., Giakoumaki, A., Argyropoulos, V. & Anglos, D. Measuring the thickness of protective coatings on historic metal objects using nanosecond and femtosecond laser induced breakdown spectroscopy depth profiling. *Spectrochim. Acta Part B At. Spectrosc*, **60**, 1163–1171 (2005).
15. Balzer, H., Hoehne, M. R., Noll, R. & Sturm, V. New approach to online monitoring of the Al depth profile of the hot-dip galvanised sheet steel using LIBS. *Anal. Bioanal. Chem*, **385**, 225–233 (2006).
16. Corsi, M. *et al.* Three-dimensional analysis of laser induced plasmas in single and double pulse configuration. *Spectrochim. Acta Part B At. Spectrosc*, **59**, 723–735 (2004).
17. Papazoglou, D. G., Papadakis, V. & Anglos, D. In situ interferometric depth and topography monitoring in LIBS elemental profiling of multi-layer structures. *J. Anal. At. Spectrom*, **19**, 483–488 (2004).
18. Kurniawan, K. H. *et al.* Hydrogen emission by Nd-YAG laser-induced shock wave plasma and its application to the quantitative analysis of zircalloy. *J. Appl. Phys*, **96**, 1301–1309 (2004).
19. Kurniawan, K. H. *et al.* The role of He in enhancing the intensity and lifetime of H and D emissions from laser-induced atmospheric-pressure plasma. *J. Appl. Phys*, **105**, 103303 (2009).
20. Kurniawan, K. H. *et al.* Detection of deuterium and hydrogen using laser-induced helium gas plasma at atmospheric pressure. *J. Appl. Phys*, **98**, 93302 (2005).
21. Hai, R. *et al.* Comparative study on self-absorption of laser-induced tungsten plasma in air and in argon. *Opt. Express*, **27**, 2509–2520 (2019).
22. Xiong, Z., Hao, Z., Li, X. & Zeng, X. Investigation on the reduction of self-absorption effects in quantitative analysis using fiber laser ablation laser-induced breakdown spectroscopy. *J. Anal. At. Spectrom*, **34**, 1606–1610 (2019).
23. Tang, Y. *et al.* Investigation of the self-absorption effect using time-resolved laser-induced breakdown spectroscopy. *Opt. Express*, **27**, 4261–4270 (2019).
24. Tang, Y. *et al.* Multielemental self-absorption reduction in laser-induced breakdown spectroscopy by using microwave-assisted excitation. *Opt. Express*, **26**, 12121–12130 (2018).

25. Li, J. M. *et al.* Self-absorption reduction in laser-induced breakdown spectroscopy using laser-stimulated absorption. *Opt. Lett*, **40**, 5224–5226 (2015).
26. Cristoforetti, G. & Tognoni, E. Calculation of elemental columnar density from self-absorbed lines in laser-induced breakdown spectroscopy: A resource for quantitative analysis. *Spectrochim. Acta Part B At. Spectrosc*, **79–80**, 63–71 (2013).
27. Aragón, C. & Aguilera, J. A. CSigma graphs: A new approach for plasma characterization in laser-induced breakdown spectroscopy. *J. Quant. Spectrosc. Radiat. Transf*, **149**, 90–102 (2014).
28. Safı, A. *et al.* Exploiting Self-Absorption for Plasma Characterization in Laser-Induced Breakdown Spectroscopy Experiments: A Comparison of Two Recent Approaches. *Anal. Chem*, **91**, 8595–8601 (2019).
29. Hao, Z. Q. *et al.* Investigation on self-absorption at reduced air pressure in quantitative analysis using laser-induced breakdown spectroscopy. *Opt. Express*, **24**, 26521–26528 (2016).
30. Fu, Y., Warren, R. A., Jones, W. B., Smith, B. W. & Omenetto, N. Detecting Temporal Changes of Self-Absorption in a Laser-Induced Copper Plasma from Time-Resolved Photomultiplier Signal Emission Profiles. *Appl. Spectrosc*, **73**, 163–170 (2019).
31. Hou, J. J. *et al.* Resonance/non-resonance doublet-based self-absorption-free LIBS for quantitative analysis with a wide measurement range. *Opt. Express*, **27**, 3409–3421 (2019).
32. Bredice, F. *et al.* Evaluation of self-absorption of manganese emission lines in Laser Induced Breakdown Spectroscopy measurements. *Spectrochim. Acta Part B At. Spectrosc*, **61**, 1294–1303 (2006).
33. Rezaei, F., Karimi, P. & Tavassoli, S. H. Estimation of self-absorption effect on aluminum emission in the presence of different noble gases: comparison between thin and thick plasma emission. *Appl. Opt*, **52**, 5088–5096 (2013).
34. Rezaei, F. *et al.* A review of the current analytical approaches for evaluating, compensating, and exploiting self-absorption in Laser Induced Breakdown Spectroscopy. *Spectrochim. Acta Part B At. Spectrosc*, **169**, 105878 (2020).
35. Hedwig, R. *et al.* Suppression of self-absorption effect in laser-induced breakdown spectroscopy by employing a Penning-like energy transfer process in helium ambient gas. *Opt. Express*, **28**, 9259–9268 (2020).
36. Karnadi, I. *et al.* Suppression of self-absorption in laser-induced breakdown spectroscopy using a double pulse orthogonal configuration to create vacuum-like conditions in atmospheric air pressure. *Sci. Rep*, **10**, 13278 (2020).
37. Pardede, M. *et al.* Unusual parallel laser irradiation for suppressing self-absorption in single pulse laser-induced breakdown spectroscopy. *Opt. Express*, **29**, 22593–22602 (2021).

Figures

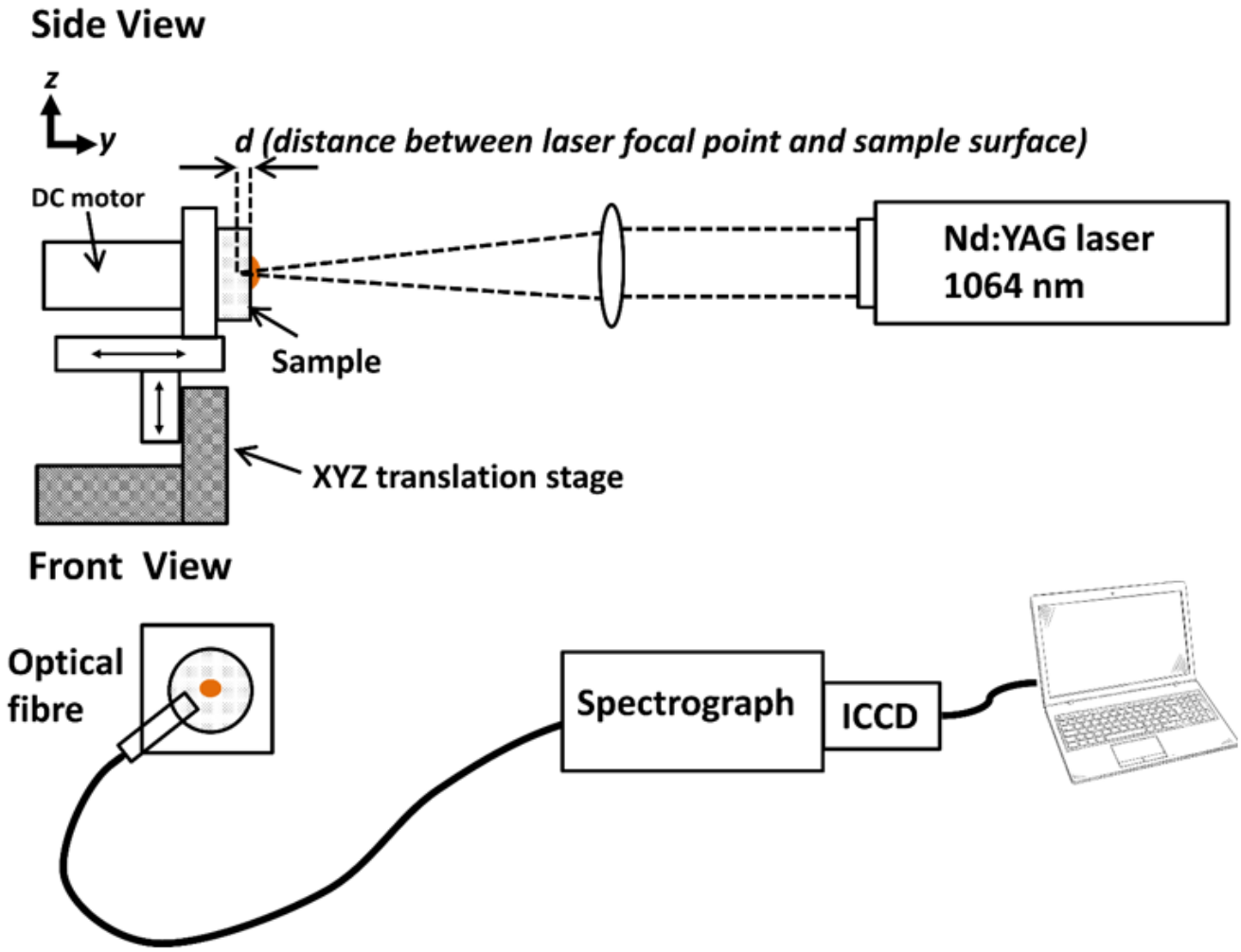

Figure 1

Diagram of the experimental set up

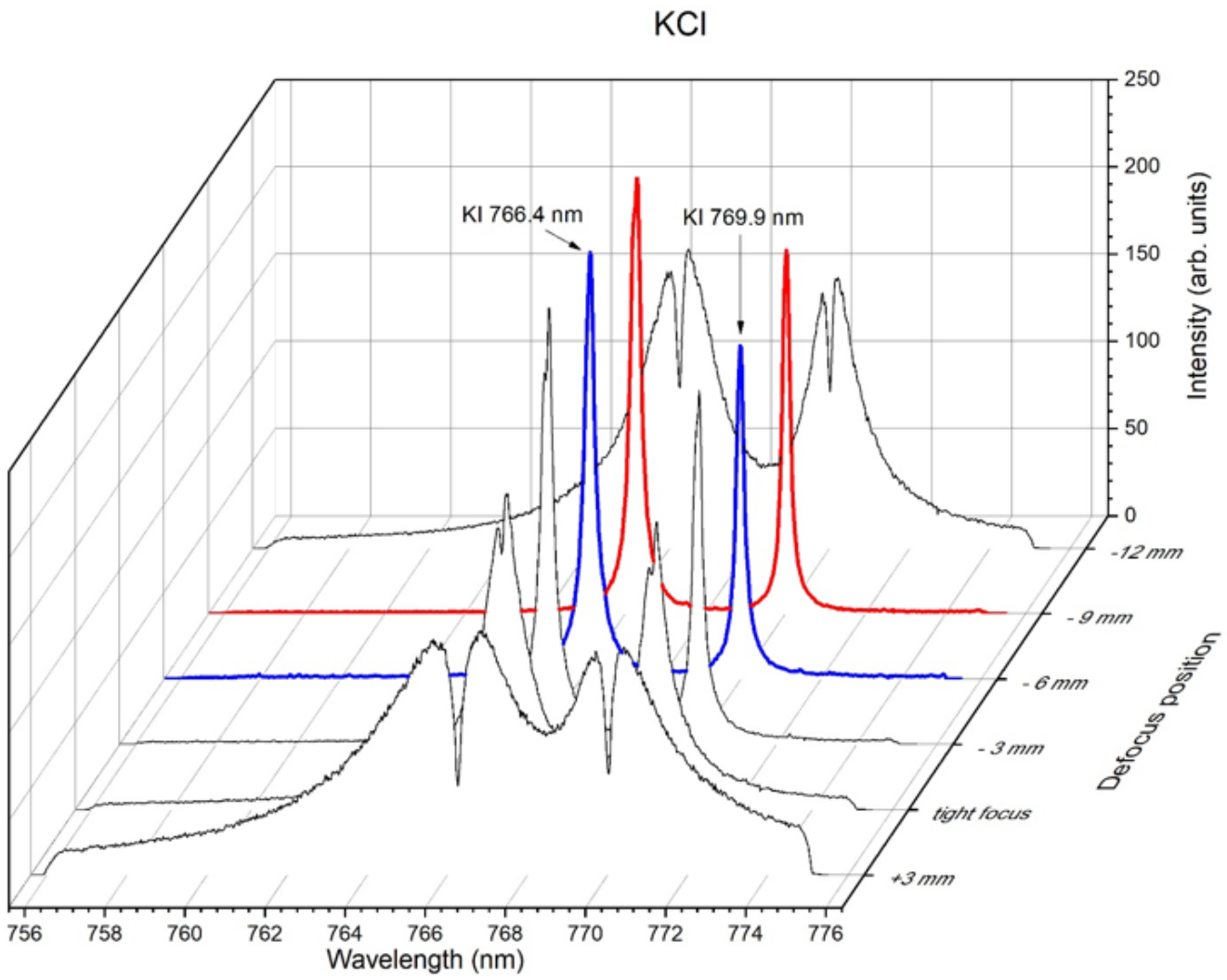

Figure 2

The emission spectra of KCl taken at different focusing position, tight focus, +3 mm, - 3mm, -6 mm, -9 mm, and -12 mm. – denotes shorter focusing position and + denotes longer focusing position. The laser energy is fixed at 21 mJ and the gate delay and gate width of the ICCD is set at 1 μs and 30 μs, respectively.

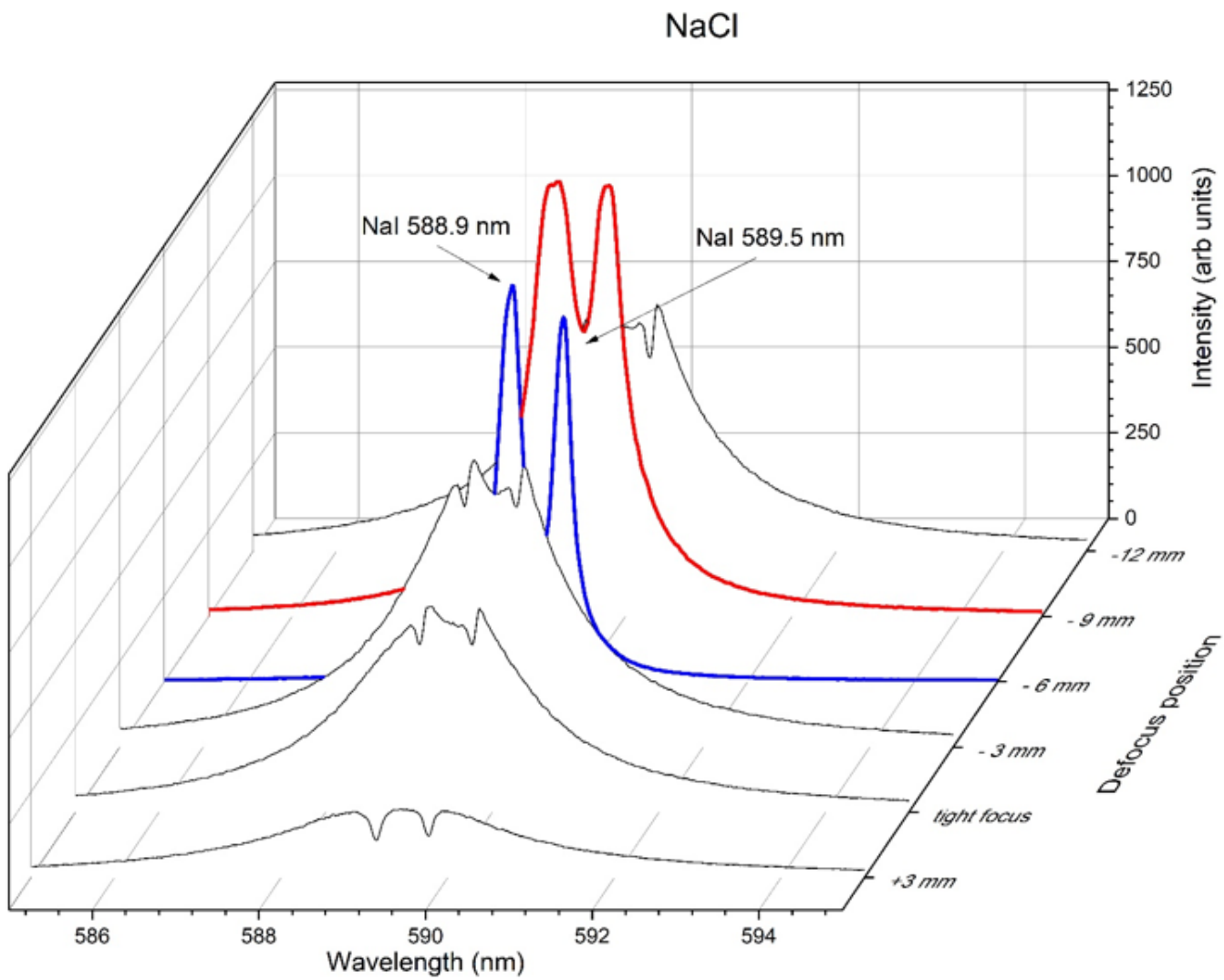

Figure 3

The emission spectra of NaCl taken at different focusing position, tight focus, +3 mm, - 3mm, -6 mm, -9 mm, and -12 mm. – denotes shorter focusing position and + denotes longer focusing position. The laser energy is fixed at 21 mJ and the gate delay and gate width of the ICCD is set at 1 μs and 30 μs, respectively.

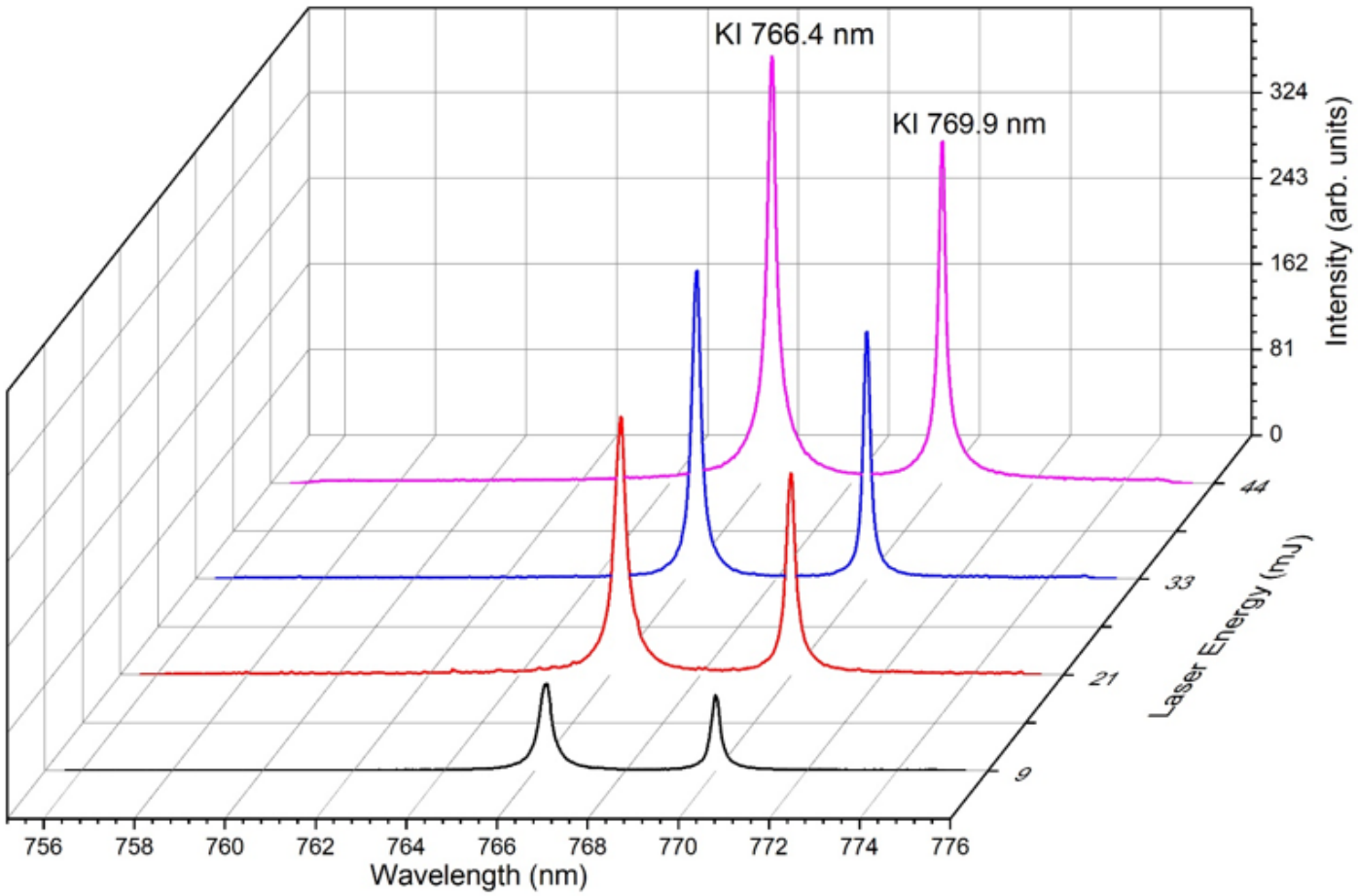

Figure 4

Emission spectra of KCl pellet under different laser energy. The focusing position is set at defocus – 6 mm. The gate delay and gate width of the ICCD is set at 1 μs and 30 μs, respectively.

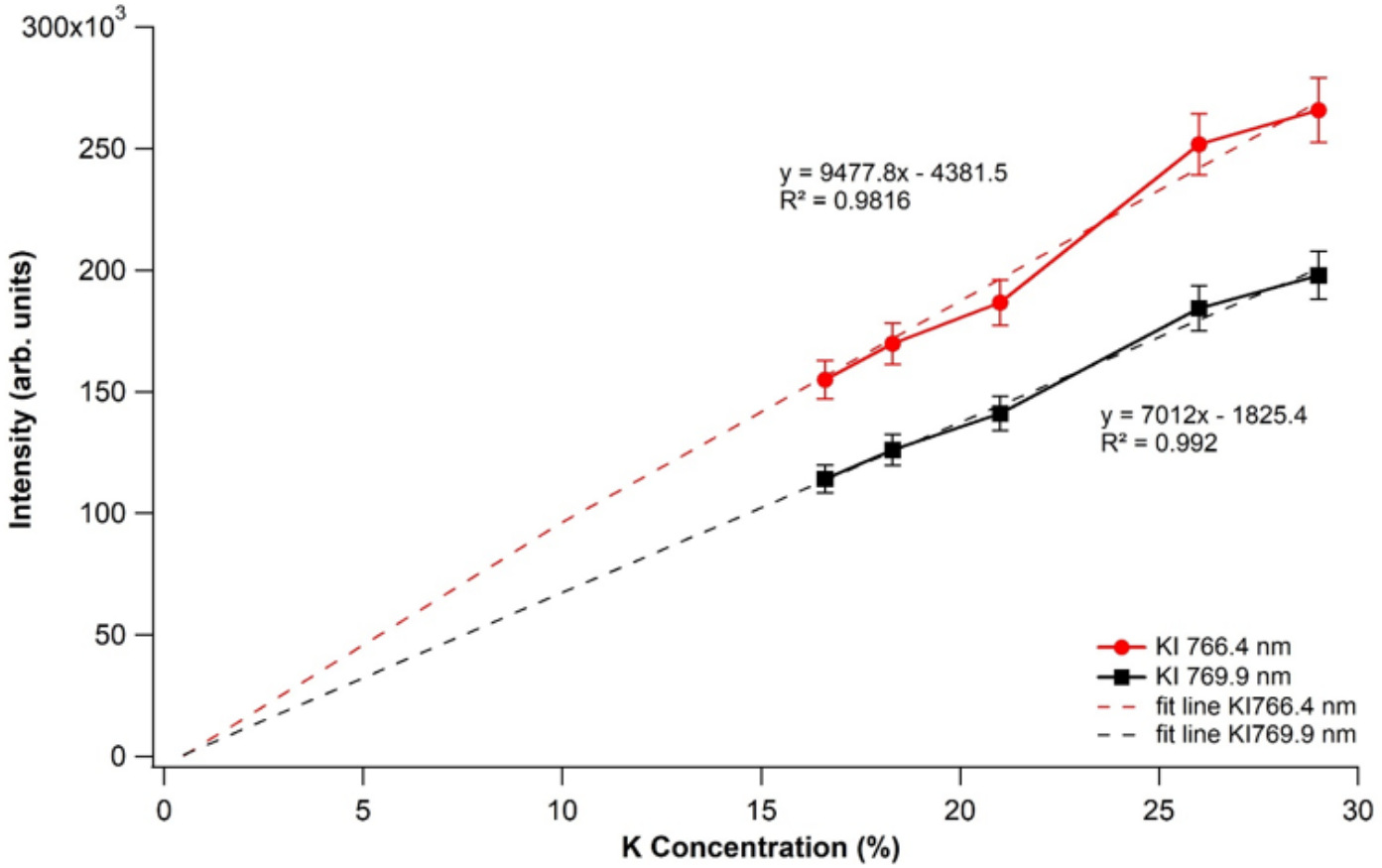

Figure 5

Plot between the emission intensity of K I 766.4 nm and K I 769.9 nm as a function of K concentration. Each data point in this figure is obtained from the average of 5 data produced each by 20 successive laser irradiations.